Utilization of Fire Dynamics Simulator Model to Study Rice Husk Gasification in Fixed-bed Gasifier

Ming-Yung Wang, Ching-Po Lin, Yi-Tseng Li, and Hsiao-Kang Ma*

Computational Fluid Dynamic (CFD) modeling applications of the biomass gasification process help to optimize the gasifier. This study aims to investigate the impact of several physical parameters on the behavior of gasification in a fixed-bed downdraft gasifier. To that end, the study presents a comparison of the results computed using the Fire Dynamics Simulator (FDS) model with experimental results of biomass gasification. Therefore, different sets of simulations and experiments have been performed to examine the effects of initial moisture content, equivalence ratio, high heating value (HHV), and cold gas efficiency (CGE). At the optimum operation, the equivalence rate is 0.3, the HHV can reach 5.71 MJ/m^3, and the produced hydrogen concentration is 26.53 vol%. For an initial moisture content of 11.18%, the measured CGE is 66.85%, which is within the range of 65.07% to 70.44%. In general, the initial moisture content of the rice husks is suggested to be below 18%. The overall results indicate that the FDS model can effectively simulate and analyze gasification performance inside the gasifier, and the performance of an improved downdraft gasifier system (IDGS) is improved by higher cold gas efficiency.

Keywords: Gasification; CFD Simulation; Biomass; FDS

*Contact information: Department of Mechanical Engineering, National Taiwan University, Taipei 106, Taiwan, R.O.C.; *Corresponding author: skma@ntu.edu.tw*

INTRODUCTION

The gasification of biomass wastes has generated more attention after the Fukushima Daiichi nuclear disaster. Nzila *et al.* (2010) evaluated the bio-waste energy potential in Kenya, which is equivalent to 73% of the country's annual power production of 5307 GWh. Ma *et al.* (2010) assessed the potential of grain-based and economy wide effects of biofuel production in China and estimated the substitution possibilities of biofuel and fossil fuels. These researchers concluded that there is still no clear understanding of how crop residues are utilized.

Today, biomass gasification is regarded as one of the key technologies for future bio-refineries in which biomass will be converted into fuel, power, and value-added chemicals. One study (LaFontaine and Zimmerman 1989) developed detailed, illustrated instructions for the fabrication and operation of a biomass gasifier unit that is capable of providing emergency fuel for vehicles. These wood gas generators need not be limited to transportation applications. Cooking stoves (Miah *et al.* 2009), district heating systems (Vallios *et al.* 2009), local cogeneration plants (Schuster 2009), and decentralized power generation (Buragohain *et al.* 2010) can also be fueled by biomass gasifiers. Agricultural waste gasification is the thermo-chemical conversion of carbonaceous material into a fuel gas through partial oxidation. Tests with different moisture contents of sugarcane leaves and bagasse in India (Jorapur and Rajvanshi 1997) indicated that combustion gas was not

obtained at all if the moisture content exceeded 25%. Jain (2006) demonstrated that the best gasifier performance was at a specific gasification rate of approximately 200 kg/hr-m^2 in five open-core throatless, batch-fed rice husk gasifier reactors. The equivalence ratio was 0.40 and the gasification efficiency was approximately 65%.

Patel *et al.* (2013) developed a computational model to investigate the performance of a downdraft gasifier under two-dimensional, laminar, and steady state conditions for biomass gasification. However, some of the simulation results lack accuracy. Wang and Yan (2008) summarized the CFD applications in biomass thermochemical conversion and system design. Singh *et al.* (2013) summarized the CFD modeling tool used to study the combustion and gasification of fuels in a fluidized bed gasifier. There is evidence that many CFD models can be used for various types of gasifiers but not the fixed-bed gasifier in three dimensions. Papadikis *et al.* (2009) suggested that a multi-dimensional pyrolysis model needed to be built instead of a two-dimensional numerical model to adequately predict pyrolysis for most situations. McGrattan *et al.* (2007, 2009) developed a three-dimensional CFD tool for the Fire Dynamics Simulator (FDS) in the fire protection field. A careful study used the Large Eddy Simulation (LES) turbulence model, and a series of sensitivity analyses were conducted with the FDS model in a tunnel fire test with forced, time-varying longitudinal ventilation (Kim *et al.* 2008). The results are in qualitative agreement with actual fire phenomena in the near-fire and downstream regions. Moreover, Abani and Ghoniem (2013) compared the performance of the LES and RANS turbulence model in an entrained flow gasifier, and found that the LES model can predict the char conversion efficiency and species distribution throughout the gasifier. Guigay *et al.* (2009) illustrated the best way to address a backdraft situation at the scene of an underventilated fire using the FDS model. The result showed that the use of positive pressure ventilation can be very effective for the venting of flammable gases. The danger of backdraft will increase significantly during the first few seconds, but decreases very quickly. Ma *et al.* (2010) experimentally examined the gasification of coal and local petroleum coke and used the experimental results to evaluate the environmental impacts with the Umberto Life Cycle Assessment (LCA) model. Shie *et al.* (2011) studied the used of rice straw from various gasification technologies to provide a potential biofuel in Taiwan by energy life cycle assessment (ELCA).

With FDS software, this study applies large eddy simulation (LES) numerical method to solve the Navier-Stoke equation for low-speed, heat-driven flow. It focuses on solid phase biomass pyrolysis converted to gas fuel and turbulent mixing with surrounding under-ventilated air. Moreover there is consideration of incomplete combustion production of smoke and heat transport from fire. The simulation result of output data shows the backdraft effect and the visual representation of fire in the gasifier by the companion program Smokeview. This technology overcomes the shortcoming of poor accuracy for the average of the flow field and reduces the enormous computational simulation by the relatively coarse mesh.

In this study, the FDS model was used to study downdraft gasifier operation and controlled parameters to improve gasification efficiency. The simulated results were compared with experimental data to create a better design. And for simulating actual situation of experiment, the rice husk fed to gasifier by batch at different time can be simulated in FDS model. Therefore the simulated results can be used to compare with the gasification efficiency from experiment.

EXPERIMENTAL

Experimental Equipment

A downdraft gasifier produces better quality gas and lower tar content than an updraft gasifier. It is suitable and convenient for agricultural rural households. A small scale downdraft gasifier was used to investigate the quality and efficiency of gas production. Previously, a commercial simple-structure fixed bed downdraft with throat gasifier was used with rice husk as fuel to build an experimental protocol. To improve leakage, bridge problems, and to reduce the amount of tar, this study designed an improved downdraft gasifier system (IDGS) with throatless design and completed the installation of airtight gaskets to reduce leakage. Moreover, a catalyst reactor improved the quality of gas production, and a vibrating grate solved the bridge phenomenon. The results indicated that IDGS increased CGE by approximately 40% compared to the previous gasifier under the same gasification conditions. The IDGS components include a feeder, downdraft gasifier, catalyst reactor, and scrubber. To understand the experimental gasifier process, several thermocouples, a flow meter, and gas sampling were used to record and control the experiment. The composition of syngas, which is produced from gasification experiments, was measured by a gas chromatograph (China Chromatography GC2000) with thermal conductivity detector. The overall experimental gasifier and peripheral equipment are shown in Fig. 1.

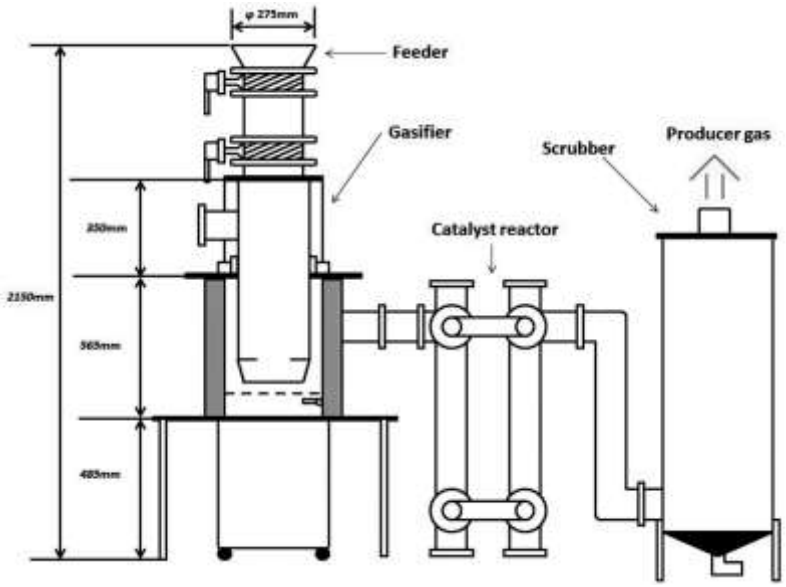

Fig. 1. Schematic of improved downdraft gasifier system (IDGS)

Experimental Procedure

In Taiwan, the annual demand for rice is approximately 1.32 million tons, including 1.26 million tons of self-produced and 140 thousand tons of imported rice. Therefore, the amount of rice husks produced is approximately 273,000 tons/year. However, only a small portion of the rice husks is used as fertilizer; the rest is burned as waste. The rice husks are not used effectively due to their unstable supply. Table 1 shows the composition of the rice husks used in this study and in other references (Yoon *et al.* 2012; Sun *et al.* 2009; Zhao *et al.* 2009; Yin *et al.* 2002).

When the experiment began, the reactor-tube was filled with 3 kg of rice husks. Then the blower was started, and some rice husks were ignited as tinder to preheat the gasifier. After a few minutes of smoky exhaust, the gas at the blower exhaust was tested by safely and carefully attempting to ignite it. When the fire spread over the rice husks in the gasifier feed, the rice husks entered from the feeder at 4.39 kg/h to a certain level of the gasifier. The feeder was closed prior to the experiment.

When the combustion zone temperature reached approximately 900 ^{o}C, the air flow rate was controlled to reach the equivalence ratio for the given experiment. After the gasifier temperature reached a steady state, gas samples were obtained and analyzed every 15 min. The temperature profile was recorded by thermocouples positioned inside the gasifier at different heights, as shown in Fig. 2.

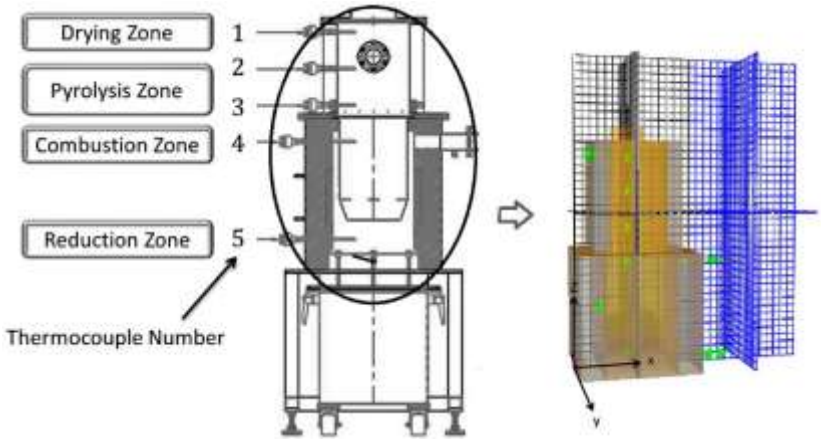

Fig. 2. Three-dimensional mesh for downdraft gasifier and thermocouple arrangement inside it

Table 1. Characteristics of Different Rice Husk

Material	Rice husk				
	Exp. Data	Yoon *et al.* 2012	Sun *et al.* 2009	Zhao *et al.* 2009	Yin *et al.* 2002
Proximate Analysis wt%					
Moisture	11.18	3.6	4.64	8.3	11.7
Volatile Matter	78.63	60	63.64	-	53.1
Ash	10.20	16.3	17.48	-	14.8
Ultimate Analysis wt%					
Carbon	40.23	38.5	37.99	37.35	36.74
Oxygen	42.68	36.6	34.66	33.19	42.55
Hydrogen	5.14	5.5	4.64	4.49	5.51
Nitrogen	0.14	0.4	0.49	-	0.28
Sulfur	0.33	0.2	0.07	-	0.55
HHV(MJ/kg)	17.2	16.58	13.78	13.67	15.7

THEORETICAL ANALYSIS

FDS Model

The FDS model, developed by the National Institute of Standards and Technology (NIST), is appropriate for low-speed, thermally driven flow, with an emphasis on heat transport from fires. In this study, the FDS model used the same outline dimensions and

cross sections as the experimental equipment but eliminated the downstream components of the gasifier. The gasifier geometry was simplified because the millions of wood gasifiers built during World War II proved that shape, form, and construction material had little or no effect on the performance of the unit (LaFontaine and Zimmerman 1989). Figure 2 shows a simulated diagram and the mesh construction of the gasifier. The total mesh size consists of 18,000 cells. The grid sizes are based on a characteristic diameter, *D** (Kim *et al.* 2008). Considering the simulation time and the quality of calculation results, *D** was given as follows:

$$D^* = \left(\frac{\dot{Q}}{\rho_\infty c_p T_\infty \sqrt{g}}\right)^{\frac{2}{5}} \approx 0.35\text{m} \quad (1)$$

where *D** is the characteristic fire diameter, $\dot{Q}$ is the heat release rate, and constant pressure specific heat, density, temperature, and acceleration of gravity are most often denoted by c_p, ρ, T, g, for which the subscript ∞ indicates by ambient conditions.

In this study, 5% (1.71 cm), 8% (2.8 cm), and 10% (3.5 cm) of *D** were chosen as cell size to form three versions of the mesh. The meshes were composed of approximately 60,750; 18,000; and 7,600 cells, respectively. The gasifier outlet velocities for the three mesh resolutions were tested for grid independency. The mesh with cell size of 2.8 cm resulted in the lowest error of 4% between experimental and simulated value.

The following general assumptions were made in the study:

(1) The flow was unsteady

(2) No-slip condition on wall surfaces

(3) The chemical reaction was faster than the time scale of the turbulence eddies

Governing equations

The equations for conservation of mass and momentum and the energy equation were given as follows:

$$\frac{\partial \rho}{\partial t} + \nabla \cdot \rho u = \dot{m}_b''' \quad (2)$$

$$\frac{\partial}{\partial t}(\rho u) + \nabla \cdot \rho u u + \nabla p = \rho g + f_b + \nabla \cdot \tau_{ij} \quad (3)$$

$$\frac{\partial}{\partial t}(\rho h_s) + \nabla \cdot \rho h_s u = \frac{Dp}{Dt} + \dot{q}''' - \dot{q}_b''' - \nabla \cdot \dot{q}'' + \varepsilon \quad (4)$$

Turbulence model

The Large Eddy Simulation (LES) model was considered for the simulation with the viscosity coefficient μ used in the LES module,

$$\mu_{ijk} = \rho_{ijk}(C_s\Delta)^2|S| \quad (5)$$

$$k_{ijk} = \frac{C_{p,0}\mu_{ijk}}{Pr_t} \; ; \; (\rho D)_{ijk} = \frac{\mu_{ijk}}{Sc_t} \quad (6)$$

where Cs is the experience constant, and the Prandtl number (Pr_t) and Schmidt number (Sc_t) are assumed to be constants. Turbulent kinetic energy is most often denoted by *k*.

Heat transfer model

The equations for the solid conductivity module, solid surface convection module, and radiation module can be given as follows:

$$\rho_s c_s \frac{\partial T_s}{\partial t} = \frac{\partial}{\partial x} k_s \frac{\partial T_s}{\partial x} + \dot{q}_s''' \quad (7)$$

$$\dot{q}_c'' = h\Delta T \ \ (W/m^2) \quad (8)$$

$$s \cdot \nabla I_\lambda(x,s) = -[\kappa(x,\lambda) + \sigma_s(x,\lambda)] I_\lambda(x,s) + B(x,\lambda) + \frac{\sigma_s(x,\lambda)}{4\pi} \int_{4\pi} \Phi(s,s') I_\lambda(x,s') ds' \quad (9)$$

Pyrolysis model

The general evolution equation for a material undergoing one or more reactions is,

$$\frac{\partial Y_{s,i}}{\partial t} = -\sum_{j=1}^{N_{r,j}} r_{ij} + \sum_{i'=1}^{N_m} \sum_{j=1}^{N_{r,i'}} v_{s,i'j} r_{i'j} \ , \ (i' \neq i) \quad (10)$$

$$Y_{s,i} = \left(\frac{\rho_{s,i}}{\rho_{s,0}}\right) \quad (11)$$

where $Y_{s,i}$ is a quantity that decreases if the *i*th component decomposes. $\rho_{s,i}$ is the density of the *i*th material component of the layer. $\rho_{s,0}$ is the initial density of the layer.

$$r_{ij} = A_{ij} Y_{s,i} exp\left(-\frac{E_{ij}}{RT_s}\right) \quad (12)$$

The quantity r_{ij} defines the rate of reaction at the temperature, T_s, of the *i*th material undergoing its *j*th reaction. The kinetic constants for the reaction are found from the formulae,

$$E = \frac{er_p}{Y_0} \frac{RT_p^2}{\dot{T}}; A = \frac{er_p}{Y_0} e^{E/RT_p} \quad (13)$$

where T_p and r_p/Y_0 are the reference temperature and rate, respectively.

In general, rice husks consist of cellulose, water, and lignin components. The cellulose is converted to active carbon by pyrolysis, using the kinetic parameters A=2.8E19, E=2.424E5. Active carbon is converted to char and fuel gases using the kinetic parameters A=1.3E10, 3.23E14 and E=1.505E5, 1.965E5, respectively, as suggested by FDS wood example. Furthermore, the water evaporated from original rice husk by A=1E20 and E=1.62E5. It was assumed that the lignin in the rice husk that does not burn, evaporate, or decompose.

Combustion model

The pyrolysis fuel gas reaction can be described by a so-called mixed-fraction combustion model for the evolution of fuel gas from its surface of origin through the combustion process. The Mixture Fraction Combustion Model was as follows:

$$C_x H_y O_z N_a M_b + v'_{O_2} O_2 \rightarrow v_{H_2O} H_2O + (v'_{CO} + v_{CO}) CO + v_s s + v_{N_2} N_2 + v_M M \quad (14)$$

$$v'_{CO} \left[CO + \frac{1}{2} O_2 \rightarrow CO_2\right] \quad (15)$$

This is a two-step reaction. The first step produces CO, and second step yields CO_2. This simulation is used for incomplete combustion reactions.

Boundary conditions

The adopted boundary conditions in simulation are listed as below:

1. Ambient air temperature and pressure were 20 ^{o}C and 101325 Pa.
2. Air inlet velocities were set with velocity inlet type and the condition was 1.01, 1.52, 2.02, 2.53, and 3.03 m/s at equivalence ratio (ER) 0.2, 0.3, 0.4, 0.5, and 0.6, respectively.
3. Syngas outlet was setting with pressure outlet type under ambient pressure condition.
4. Inside and outside wall material were sheet metal, and the medium material was filled with rock wool for insulation. The specific heat, conductivity, and density were assigned for each material, respectively.

Parameter Definition

Equivalence ratio (ER), Φ

The definition of equivalence ratio (ER) is the actual AF ratio (air to fuel ratio) to the stoichiometric AF ratio, as shown in Eq. 16:

$$\Phi = \frac{Actual\ Air\ to\ Fuel\ Ratio}{Stoichiometric\ Air\ to\ Fuel\ Ratio} \quad (16)$$

Gas production rate

Because the gasifier temperature (even in the oxidation zone) is less than 1200 ^{o}C and hypoxic combustion occurs without a dramatic change in pressure, generation of free NOx can be assumed. In other words, nitrogen does not participate in the reaction. Therefore, the definition of Gas Production Rate is shown in Eq. 17 as

$$Gas\ Production\ Rate = \frac{79\%}{XN_2} \times Air\ Flow\ Rate \quad (17)$$

Cold gas efficiency (CGE)

An important characteristic value that is valid for all gasification processes for any fuel is the degree of Cold Gas Efficiency (CGE). With this value, it is possible to compare the efficiency of various gasification processes. The calculation of Cold Gas Efficiency is defined in Eq. 18.

$$Cold\ Gas\ Efficiency = \frac{HHV_{gas} \times gas\ production\ rate}{HHV_{biomass} \times biomass\ fedding\ rate} \times 100\% \quad (18)$$

RESULTS AND DISCUSSION

Simulation Results from FDS Model

The FDS model can clearly simulate the process of drying, pyrolysis, and incomplete combustion, due to oxygen-deficient combustion. The pyrolysis process produces many combustible gases, and some of them will escape from the outlet. If there is no suitable storage system for the outlet combustible gas, then the high-temperature flammable gas may immediately burn with oxygen in the environment, and this

phenomenon is similar to fire disasters. To allow better visualization, the ignition and feeding of the rice husks into the gasifier are shown in a 3D view of the gasifier, as indicated in Fig. 3a. Figure 3b shows that the flammability region propagated, became reduced in width, and moved toward the top of the gasifier. The wider the flammability region, the more likely it is that fuel gas could come in contact with a high-temperature source (*e.g.*, smoldering fire) and create a backdraft phenomenon (Guigay *et al.* 2009). The exhaust fan attracted the fuel gas to concentrate within the flammable region where the temperature was approximately 500 ^{o}C, which is why the flame was observed to spread at the exhaust duct outlet when oxygen was sufficient.

Figure 3c shows the pressure contours in gasification process and demonstrates that the initial pressure was approximately 0 gauge pressure. After around 10 min, the result shows the gasifier pressure slightly rose to drive production air. While the temperature attained 800 ^{o}C and the gasification reaction tended to steady state, the pressure grew rapidly and the gasifier pressure reached approximately 750 to 1800 gauge pressure. Figure 3d shows the result of gasifier air velocity, which reveals that the initial velocity presented an unsteady state while feeding. And when the amount of feeding rate attained the experiment needs, the airflow became stable and velocity was enhanced to 1.5 m/s by gasifier pressure. The gasifier reaction in initial state can be described clearly by FDS simulation model.

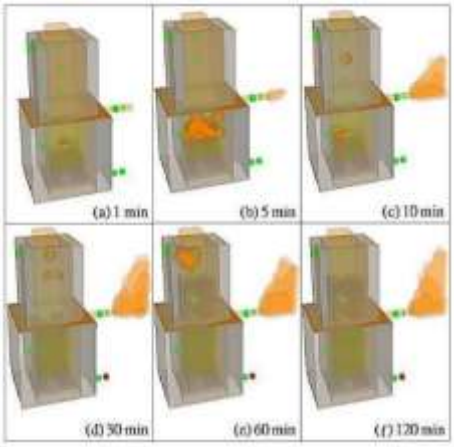

Fig. 3a. Gasification phenomenon in gasifier

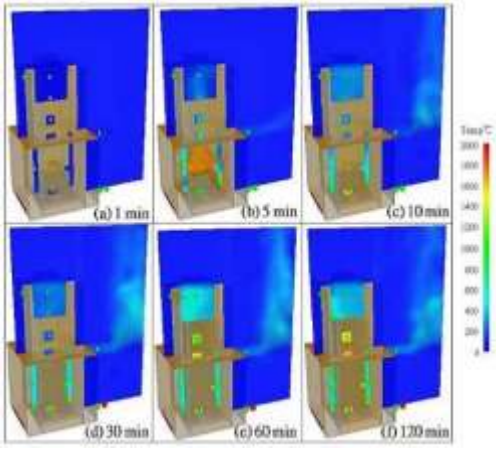

Fig. 3b. Temperature contours in gasifier at different time

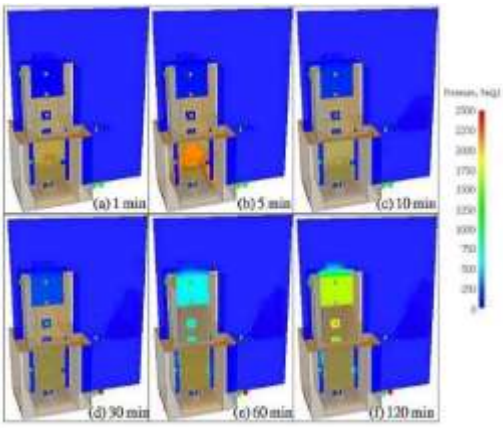

Fig. 3c. Pressure contours in gasifier at different time

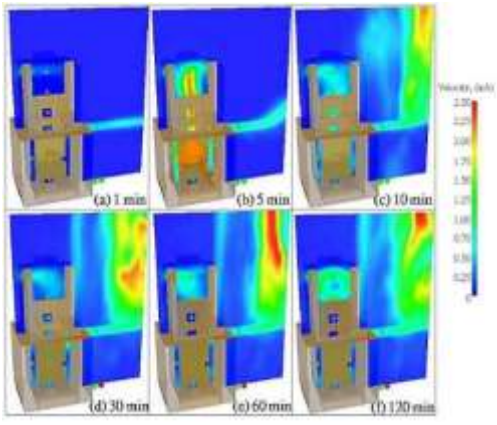

Fig. 3d. Velocity contours in gasifier at different time

Comparison of the Effect of Air Inlets on the Difference Equivalence Ratio (ER), Φ

In Eq. 16, the stoichiometric AF ratio is calculated by the amount of air required for complete combustion of rice husks. The actual AF ratio is the supply rate of air flow divided by the rate of fuel consumption in the experiment. The rate of fuel consumption is the total feeding amount over the experimental time, but in FDS that will directly simulate the burning rate of the rice husks. Controlled air supply was considered in this study. The difference equivalence ratio for the experimental results and the FDS model simulations are shown in Table 2.

The results show that simulated air inlet values almost matched the measured data when the rice husk burning rate in the FDS program was equal to the feeding rate of experiment. Furthermore, the actual air fuel ratios are almost equivalent.

Table 2. Comparison of Measured and Simulated A/F Ratio at the Same Equivalence Ratio

Equivalence Ratio Φ	Feeding Rate (kg/h)	Measured Result		Simulated Result	
		Air inlet (L/min)	A/F ratio	Air inlet (L/min)	A/F ratio
0.2	4.39	56.39	0.908	54.24	0.869
0.3	4.39	84.57	1.362	82.2	1.320
0.4	4.39	112.78	1.816	110.4	1.795
0.5	4.39	140.96	2.27	139.8	2.262
0.6	4.39	169.17	2.724	168.00	2.730

Comparison of Gas Production with Different ERs

In FDS, setting the outflow velocity at the exhaust outlet is based the conservation of mass. To calculate, the inlet airflow mass plus the burned away mass of the rice husks will equal the outlet production fuel gas flow mass. The simulation results were analyzed to verify that the model conserves mass. This study does not consider the effect of air leakage. A comparison of the gas production rate with different ERs is shown in Fig. 4.

The results show good simulation when ER=0.3, but over-prediction of gas production rate when ER=0.2 and under-prediction of gas production rate when ER=0.5 and 0.6. The maximum error in the gas production rate was less than 20%. In this study, Eq. 17 was used to calculate the gas production rate because the organic compounds are still contained in the producer gas after the conversion of pyrolysis vapors in the hot oxidation zone to tar compounds. Meanwhile the minimum straight pipe distance requirement of flow meter cannot meet because of the influence of valves, elbows, tees, *etc*., which is typically 10 to 20 diameters upstream and 5 diameters downstream for relatively clean fluids. This requirement can increase with the process solid concentration or composition. Additionally, the requirement will affect the downstream flowmeter accuracy in non-homogeneous situations (Liptak 2003). Moreover, the gasifier oxidation zone temperature is less than 1200 ^{o}C, and hypoxia combustion occurs without a significant change in pressure. In this study, free NO_X generation was assumed.

Organic compounds and minimum straight pipe requirement also affect the flowmeter accuracy to evaluate the difference between the simulation results and the experimental results.

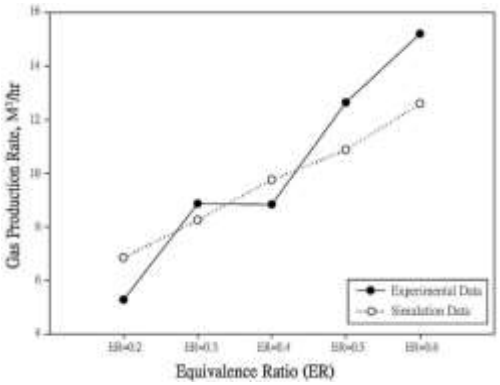

Fig. 4. Comparison of gas production rate at different equivalence ratio

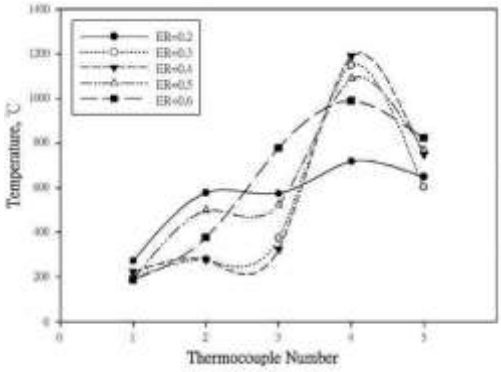

Fig. 5. Temperature profile measured throughout the experiment by thermocouples

Comparison of Temperature Profiles

In this experiment, the axial temperature distribution of the experiment gasifier was recorded by a thermocouple. The temperature distribution curves at different equivalence ratios are shown in Fig. 5. The calculation results indicate that the No. 1 thermocouple was in the drying zone, with temperatures approximately 100 ^{o}C to 200 ^{o}C. In this zone, the moisture in the rice husks was evaporated, and they were brought to the reduction zone. The No. 2 and No. 3 thermocouples were in the pyrolysis zone, where the temperature was between 200 ^{o}C to 600 ^{o}C. The biomass was pyrolyzed to tar, volatile compounds, and char residues in this zone, leading to a larger temperature gradient. The No. 4 thermocouple was in the combustion zone (approximately 800 ^{o}C to 1100 ^{o}C), and it provides energy for the reduction zone and pyrolysis zone. The No. 5 thermocouple is located in the reduction zone. The temperature of this zone was 600 ^{o}C to 900 ^{o}C. At Φ =0.2, Fig. 8 shows that the temperature profile was lower than other equivalence ratio. This temperature reduction was most likely observed because less-intense combustion and endothermic gasification cause a decrease in temperature.

As shown in Table 3, the concentration trend of hydrogen first increased and then dropped with the increase in the equivalence ratio. At Φ = 0.2, the concentration of hydrogen was 9.6 vol%, which may have been caused by the lack of an air inlet. At Φ = 0.3, the concentration increased to 26.53 vol%. After Φ = 0.3, it exhibited a downward trend because of excessive air inflow. The concentration of carbon monoxide and methane had an apparent downward trend with the increase in the equivalence ratio. The highest concentrations of carbon monoxide and methane were 12.07 vol% and 2.21 vol%, respectively.

Table 3. Composition of Production Gas, Vol% at Different Equivalence Ratio

Equivalence Ratio Φ	N_2	H_2	CH_4	CO
0.2	50.77	9.60	2.21	12.07
0.3	45.29	26.53	2.06	11.90
0.4	60.47	14.39	1.91	8.77
0.5	52.88	9.48	1.63	8.76
0.6	52.78	7.31	1.61	8.55

The High Heating Value (HHV) is calculated by using each heating value of the gas composition. The main factors affecting the HHV are H_2, CO, and CH_4, which were 12.75, 12.63, and 38.82 MJ/m^3, respectively. The HHV calculated in the experiment is 5.71 MJ/m^3. In FDS, the HHV was substituted for the Heat Release Rate (HRR), which counts the gas molecules formed in the combustion process.

Influence of Initial Moisture Content of Rice Husks

The previous results show that a well-executed experiment with ER=0.3, and the FDS model can simply and quickly predict the cold gas efficiency and heat release rate with different initial moisture contents in biomass. Figure 6 shows the variation in HRR and CGE with different initial moisture contents in rice husks. Figure 6 demonstrates that as the initial moisture content in rice husk increased, the HRR and CGE changed slightly, but when the initial moisture content was over 18%, the HRR and CGE dropped abruptly. One may deduce that too high an initial moisture content prevents the temperature in the gasifier from reaching that required for the gasification reaction, so the production of fuel gas decreases. For an initial moisture content of 11.18%, the measured CGE is 66.85%, which is within the range of 65.07% to 70.44% simulated by the FDS model.

The fuel mass fraction is the normalized density of the material of fuel in syngas, which increases as the gasifier is heated continually until reaching steady state. This curve is shown in Fig. 7. When studying the values over the first 50 minute, there was a very intense evolution. This is because the temperature rise from ambient to gasification temperature leads to pyrolysis of the rice husk as well as to gasification very quickly.

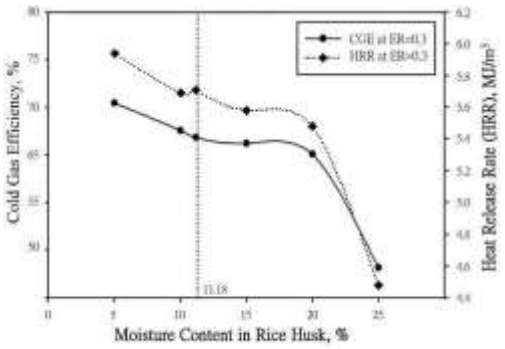

Fig. 6. The variation of HRR and CGE with different moisture content in rice husk

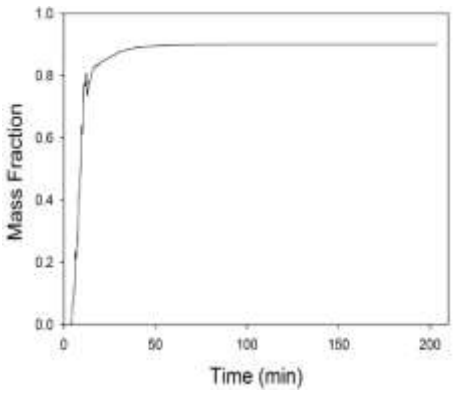

Fig. 7. The fuel mass fraction in syngas increases with time curve

CONCLUSIONS

This study evaluated the performance of rice husk gasification and the feasibility of the FDS model to simulate the process in the improved downdraft gasifier system (IDGS). The FDS model can clearly simulate the cold gas efficiency (CGE) and heat release rate (HRR) and demonstrates the phenomena that occur in the gasification process of drying, pyrolysis, and incomplete combustion. The major conclusions are as follows:

1. The optimum operation of the improved gasifier (IDGS) was found when the equivalence rate was ER=0.3, the HHV reached 5.71 MJ/m^3, and when the produced hydrogen concentration was 26.53 vol %.

2. The simulated gas production rate exhibits a similar pattern to the measured data, and the maximum error was less than 20%.
3. At ER=0.3, the simulated CGE is 66.72%, which is in agreement with the experimental value of 66.85%. Compared with other results, the performance of the IDGS has been improved with higher cold gas efficiency.
4. The FDS model can simply and quickly predict the cold gas efficiency and heat release rate under different initial moisture contents in biomass. For an initial moisture content of 11.18%, the measured CGE is 66.85%, which is within the range of the simulated result of 65.07% to 70.44%. In general, the initial moisture content of rice husks should be below 18%.

ACKNOWLEDGMENTS

This study represents part of the results obtained under the support of National Science Council, Taiwan, ROC (Contract No. NSC102-3113-P-002-038).

REFERENCES CITED

Abani, N., and Ghoniem, A. F. (2013). "Large eddy simulations of coal gasification in an entrained flow gasifier," *Fuel* 104, 664-680.

Buragohain, B., Mahanta, P., and Moholkar, V. S. (2010). "Biomass gasification for decentralized power generation: The Indian perspective," *Renew. Sust. Energ.* 14(1), 73-92

Guigay, G., Gojkovic, D., Bengtsson, L. G., Karlsson, B., and Eliasson, J. (2009). "The use of CFD calculations to evaluate fire-fighting tactics in a possible backdraft situation," *Fire Technol.* 45, 287-311.

Jain, A. K. (2006). "Design parameters for a rice husk throatless gasifier," *The CIGR Ejournal* 8, 1-13.

Jorapur, R., and Rajvanshi, A. K. (1997). "Sugarcane leaf-bagasse gasifiers for industry heating applications," *Biomass Bioenerg.* 13(3), 141-146.

Kim, E., Woycheese, J. P, and Dembsey, N. A. (2008). "Fire dynamics simulator (Version 4.0) simulation for tunnel fire scenarios with forced, transient, longitudinal ventilation flows," *Fire Technol.* 44, 137-166.

LaFontaine, H., and Zimmerman, F. P. (1989). *Construction of a Simplified Wood Gas Generator for Fueling Internal Combustion Engines in a Petroleum Emergency*, Federal Emergency Management Agency Washington, D.C.

Liptak, B. G. (2003). *Process Measurement and Analysis, Instrument Engineers' Handbook* 4rd Ed., Chilton Book Company, Pennsylvania.

Ma, H., Oxley, L., Gibson, J., and Li, W. (2010). "A survey of China's renewable energy economy," *Renew. Sust. Energ.* 14(1), 438-445.

Ma, H. K, Chen, B. R, Chen, S. W., Wang, M. Y, Shen, C. H, and Hsu, H. W. (2010). "Environmental impact study and life cycle assessment of a coal-petroleum coke gasification process," Poster Session. *33rd International Symposium on Combustion* Beijing China, 2-6.

McGrattan, K., Klein, B., Hostikka, S., and Floyd, J. (2007). *Fire Dynamics Simulator (Version 5) User's Guide. National Institute of Standards and Technology*, NIST Special Publication 1019-5.

McGrattan, K., Baum, H., Hostikka, Floyd, S., and J. R. Rehm. (2009). *Fire Dynamics Simulator (Version 5) Technical Reference Guide Volume 1: Mathematical Model. National Institute of Standards and Technology*, NIST Special Publication 1018-5.

Miah, Md. D., Rashid, Al. H., and Shin, M. Y. (2009). "Wood fuel use in the traditional cooking stoves in the rural floodplain areas of Bangladesh: A socio-environmental perspective," *Biomass Bioenerg.* 33(1), 70-8.

Nzila, C., Dewulf, J., Spanjers, H., Kiriamiti, H., and Langenhove, van H. (2010). "Biowaste energy potential in Kenya," *Renew. Energ.* 35(12), 2698-2704.

Papadikis, K., Gerhauser, H., Bridgwater, A.V., and Gu, S. (2009). "CFD modelling of the fast pyrolysis of an in-flight cellulosic particle subjected to convective heat transfer," *Biomass Bioenerg.* 33(1), 97-107.

Patel, D. K., Shah, N. K., and Patel, R. N. (2013). "CFD Analysis of spatial distribution of various parameters in downdraft gasifier," *Procedia Engineering* 51, 764-769.

Schuster, T. (2009). "Design and operation of a local cogeneration plant supplying a multi-family house (9.5kw electrical / 35kw thermic power) - A field report," International Conference on Renewable Energies and Power Quality. Capri: Italy, 9-11.

Shie, J. L, Chang, C. Y., Chen, C. S., Shaw, D. G., Chen, Y. H., Kuan, W. H., and Ma, H. K. (2011). "Energy life cycle assessment of rice straw bio-energy derived from potential gasification technologies," *Bioresour. Technol.* 102(12), 6735–6741.

Singh, I. R., Brink, A., and Hupa, M. (2013). "CFD modeling to study fluidized bed combustion and gasification," *Appl. Therm. Eng.* 52, 585-614.

Sun, S., Zhao, Y., Ling, F., and Su, F. (2009). "Experimental research on air staged cyclone gasification of rice husk," *Fuel Process. Technol.* 90, 465-471.

Vallios, I., Tsoutsos, T., and Papadakis, G. (2009). "Design of biomass district heating system," *Biomass Bioenerg.* 33(4), 659-678.

Wang, Y., and Yan, L. (2008). "CFD studies on biomass thermochemical conversion – Review," *Int. J. Mol. Sci.* 9, 1108-1130.

Yin, X. L, Wu, C. Z., Zheng, S. P., and Chen, Y. (2002). "Design and operation of a CFB gasification and power generation system for rice husk," *Biomass Bioenerg.* 23, 181-187.

Yoon, S. J, Son, Y. I., Kim, Y. K., and Lee, J. G. (2012). "Gasification and power generation characteristics of rice husk and rice husk pellet using a downdraft fixed-bed gasifier," *Renew. Energ.* 42, 163-167.

Zhao, Y., Sun, S., Tian H., Qian J., Su, F., and Ling F. (2009). "Characteristics of rice husk gasification in an entrained flow reactor," *Bioresource Technol.* 100, 6040-6044.

Article submitted: January 13, 2014; Peer review completed: April 12, 2014; Revised version received and accepted: May 1, 2014; Published: May 6, 2014.